Available online at www.sciencedirect.com

ScienceDirect

Procedia CIRP 94 (2020) 499–504

www.elsevier.com/locate/procedia

11th CIRP Conference on Photonic Technologies [LANE 2020] on September 7-10, 2020

Real-time monitoring of fiber laser cutting of thick plates by means of photodiodes

Nikita Levichev*, Gonçalo Costa Rodrigues, Joost R. Duflou

Department of Mechanical Engineering, KU Leuven, Celestijnenlaan 300B, Heverlee 3001, Belgium, Member of Flanders Make

* Corresponding author. Tel.: +3216377434. *E-mail address:* nikita.levichev@kuleuven.be

Abstract

Adaptive real-time monitoring and control is a natural solution for automated unmanned laser cutting that has been intensively studied for the last decades. However, sensor solutions for laser cutting are rarely used in practice. In this paper, a coaxial photodiode-based monitoring system has been developed and investigated for 4 kW fiber laser cutting of mild and stainless steel thick plates. Based on the obtained results, the feasibility of industrial application of the implemented setup is discussed.

© 2020 The Authors. Published by Elsevier B.V.
This is an open access article under the CC BY-NC-ND license (http://creativecommons.org/licenses/by-nc-nd/4.0/)
Peer-review under responsibility of the Bayerisches Laserzentrum GmbH

Keywords: Laser cutting; Fiber laser; Sheet metal; Process monitoring; Optical sensor

1. Introduction

Laser cutting is a well-established industrial process for sheet metal applications. However, cutting of thick plates is still a problem because of the characteristic limited process parameter window. Adaptive real-time monitoring and control is a natural solution but the majority of previous studies were focused on the design of monitoring systems for CO_2 laser cutting using acoustic sensors [1], photodiodes [2] or camera systems [3]. Nowadays, cutting by means of fiber lasers has become dominant and, therefore, tailored solutions are required in such systems for industrial applications.

Real-time monitoring systems have been widely investigated for a variety of laser processes [4], such as laser welding [5], additive manufacturing [6] and laser cladding [7]. In contrast to other processes, monitoring solutions for laser cutting are scantily presented in the literature, especially for near-infrared lasers. A photodiode-based cutting interruption sensor has been introduced [8] and evaluated for burr formation detection for cutting steels in the thickness range of up to 3 mm [9]. Furthermore, a cross-correlation algorithm for an InGaAs and Si photodiode-based sensor system that allows detection of cut interruption has been reported in [10]. A coaxial photodiode-based monitoring system has been implemented for piercing optimization [11]. Optical pyrometry has been used in order to detect the fluctuations of the brightness temperature of the cutting front [12]. An optical setup, based on two Si photodiodes collecting radiation from both sides of the plate, has been presented for in-situ quality assurance [13].

The development of a robust real-time monitoring system could become an important step forward towards fully automated laser cutting. The information obtained from this monitoring system could be used as input for a control system that adapts the cutting parameters during the process [14].

As already mentioned, the laser cutting of thick plates ($\geq$ 10 mm) differs from the processing of thin sheets. The dimensions and dynamics of the cutting front are significantly different. At the same time, the cut quality by way of the equilibrium between process parameters is highly sensitive to the process fluctuations, e.g. thermal focus shift, deviations in thickness, material microstructure and chemical composition.

Within this paper, a developed coaxial photodiode-based monitoring system is investigated in depth for fiber laser cutting of 15 mm mild steel plates. Quality deteriorations

2212-8271 © 2020 The Authors. Published by Elsevier B.V.
This is an open access article under the CC BY-NC-ND license (http://creativecommons.org/licenses/by-nc-nd/4.0/)
Peer-review under responsibility of the Bayerisches Laserzentrum GmbH
10.1016/j.procir.2020.09.171

caused by speed changes as well as by the heat accumulation effects are examined. Moreover, experiments with both stainless steel and mild steel for different plate thicknesses have been performed. Eventually, the feasibility of industrial application of the implemented monitoring setup is discussed.

2. Experimental setup

2.1. Laser cutting

The experiments were performed on a commercial 2D flat-bed laser cutting machine with a 4 kW IPG Ytterbium multimode fiber laser source emitting at 1.07 µm wavelength. The laser beam is delivered from a 100 µm core optical fiber into a Precitec ProCutter laser head equipped with a 200 mm focusing lens and a 100 mm collimation lens. The beam parameter product and the beam waist diameter were measured by means of an Ophir BeamWatch device as 2.84 mm mrad and 224 µm, respectively.

Table 1 provides the chemical composition of the hot rolled 15 mm mild steel plates used during the experiments according to the Certificate 3.1 (DIN-EN-10204). Three grades with different characteristics were selected, such as S355MC, both standard as well as pickled and oiled, which have the same chemical composition, and Ympress 250C laser quality. In order to test the monitoring system, thinner S355MC mild steel and 304L stainless steel plates were used as well.

Table 1. Chemical composition (wt. %) of the 15 mm plates being used.

Grade	C	Mn	Cu	Cr	Ni	Al	Si	Fe
S355MC	0.057	1.31	0.036	0.021	0.017	0,040	0.012	rest
Ympress 250C	0.148	0.90	0.016	0.025	0.017	0.043	0.004	rest

Table 2 lists process parameters obtained from the machine supplier that were used for cutting experiments. As an assist gas, oxygen of 99.95 % and nitrogen of 99.999 % purity were used for cutting of mild and stainless steel, respectively. The cutting was performed with a laser power of 4 kW and a duty cycle of 100 %.

Table 2. Process parameters for material-thickness combinations being used.

Parameter	Mild steel 8 mm	Mild steel 10 mm	Mild steel 15 mm	Stainless steel 10 mm
Speed [mm/min]	2000	1700	1100	1000
Focus position [mm] (positive is above the plate)	+4.5	+4.5	+5.5	-9.3
Nozzle diameter [mm]	1.2	1.2	1.5	3.5
Assist gas pressure [bar]	0.5	0.5	0.6	16
Stand-off distance [mm]	1.2	1.2	1.2	0.4

2.2. Monitoring system

A coaxial monitoring setup, schematically represented in Fig. 1, was built by replacing a conventional laser head mirror by a dichroic one that transmits towards the sensor the radiation with a wavelength shorter than 800 nm and longer than 1200 nm as schematically shown in Fig. 2. Then, a diaphragm with a diameter of 1.5 mm was used to decrease the optical aberrations after the laser head optics designed for the laser beam wavelength. After the diaphragm, an OD 6 notch filter was placed to remove the scattered and reflected laser radiation, which is significantly higher than the thermal radiation from the process zone, even after passing the dichroic mirror.

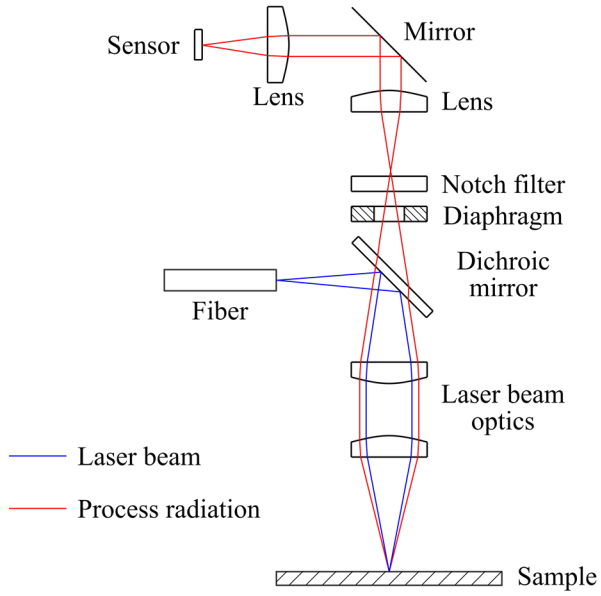

Fig. 1. Optical setup for monitoring system.

During cutting, the temperature of the process zone is higher than the melting point of steel, which is typically around 1800 K, resulting in maximum emission between 800 nm and 2000 nm according to Planck's law. Two types of photodiodes, the responsivity of which is shown in Fig. 2, were found suitable for this range: a Si photodiode, mainly sensitive in the visual spectral range from 350 to 1100 nm, and an InGaAs photodiode, responsive to the near-infrared radiation with wavelengths from 800 to 1700 nm. Since the radiation peak of the process temperatures is around 1500 nm, an InGaAs photodiode (FGA21) was selected.

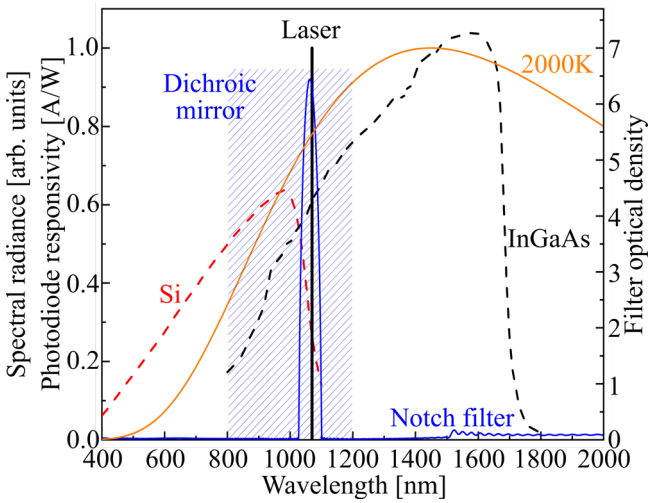

Fig. 2. Spectral characteristics of the setup: responsivity of photodiodes, optical density of the notch filter, spectral radiance of a black body with 2000 K. The laser wavelength and the non-transmitting zone of the dichroic mirror are shown approximately.

The photodiode signals were recorded by means of a data acquisition card with a sample rate of 50 kHz. Appropriate signal amplification and low pass filtering were applied. The obtained data were processed in MATLAB using a moving average to reduce the noise.

The cutting process was also analyzed by means of a Xenics Bobcat-3754 infrared camera that replaced the photodiode in the monitoring setup. An integration time of 50 µs and a frame rate of 40 fps were used for the recordings.

2.3. Evaluation methods

A Keyence Digital Microscope VHX-6000 was used for high-resolution imaging of cut edge profiles. The surface roughness of cut edges (Rz) was measured by means of a Mitutoyo Formtracer CS-3200 using a Gaussian filter with a sample length of 2.5 mm and a cut-off of 0.008 mm. The measurements of each specimen were performed for five lines with an evaluation length of 12.5 mm. The measuring lines were spaced by 3.25 mm starting at 1 mm from the top surface. The average roughness value was calculated as a mean value of these five measurements.

3. Results and discussion

The photodiode signal during both piercing and cutting of a line is shown in Fig. 3. The full penetration has been achieved after three laser pulses and is accompanied by a significant drop of the signal. Although the laser was still on for a second after the full penetration, passing some energy to the plate, the signal dropped to a much lower value. The piercing end is characterized by reaching a negligible level of the signal. The cutting is described by a constant but noisy signal. In addition to the measurement noise, increased due to the signal amplification, there is the process noise caused by the melt flow dynamics of the cutting front [15]. In order to reduce the noise, the signal was smoothed by means of a Savitzky-Golay filter resulting in the processed signal which was used for further evaluation and comparison of all experiments.

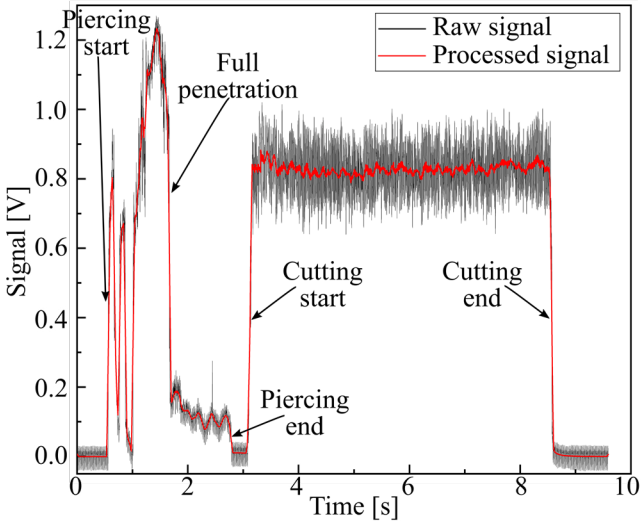

Fig. 3. Photodiode signal during piercing and cutting of a 15 mm S355MC plate.

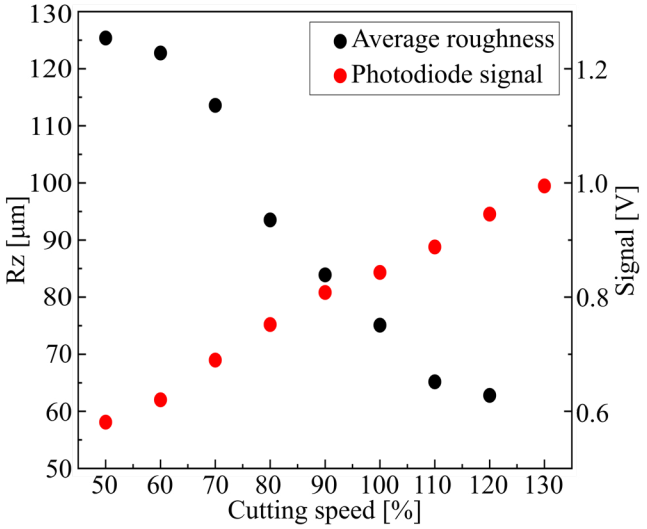

Fig. 4. Average roughness and photodiode signal during cutting of a 15 mm S355MC plate with different cutting speeds.

The average photodiode signals during straight line cutting at the nominal speed (100 %) as well as at higher and lower speeds are shown in Fig. 4. Moreover, roughness values were measured for every sample except 130 % where the edge quality drastically deteriorated causing dross occurrence that made measurement difficult and inappropriate. The change in cutting speed is clearly reflected in the cutting quality, in particular roughness, whereas the signal level is significantly higher when the cutting speed is increased.

Next to the signal level, the signal standard deviation depicted in Fig. 5 also provides useful information concerning the cutting process status. Since different behaviour of the standard deviation can be observed, the data are provided for a 1 s interval in the middle of the cutting line. When the process is seriously destabilized by the occurrence of burning defects since the energy input is too high or the cutting speed is too slow, a significant increase and variability of standard deviation can be noticed that corresponds to high roughness. Since the cutting front stability is the main factor affecting standard deviation, cutting too fast cannot be distinguished by this sensing parameter.

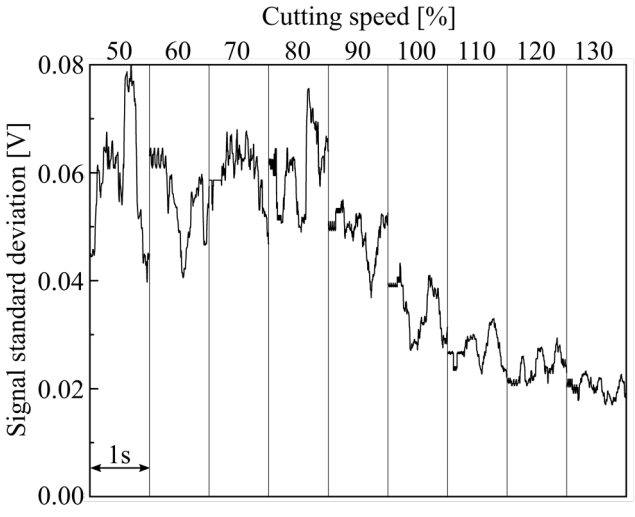

Fig. 5. Signal standard deviation during cutting of a 15 mm S355MC plate with different cutting speeds.

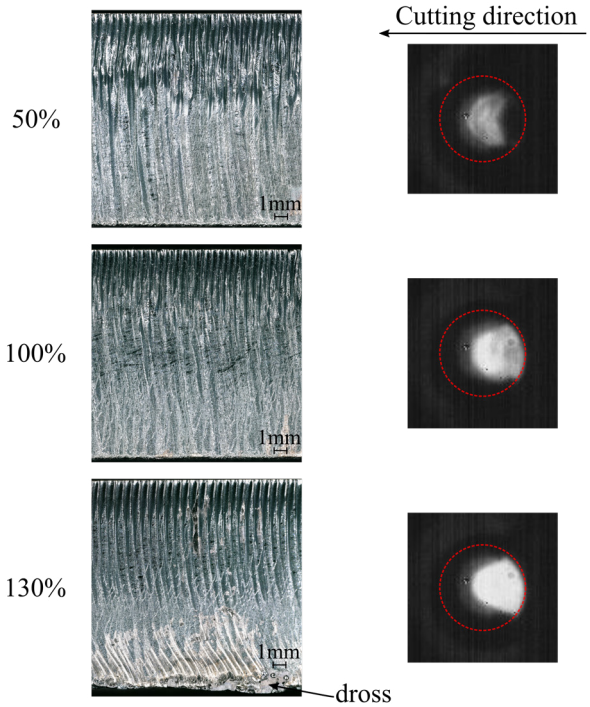

Fig. 6. Cut edges obtained during cutting of a 15 mm S355MC plate with different cutting speeds and the corresponding near-infrared camera images. The red circle indicates the nozzle border.

The cut edge profiles obtained during cutting with nominal and two extreme speeds, as well as corresponding images from the infrared camera, are shown in Fig. 6. The cut edge with a cutting speed of 100 % is characterized by a typical striation pattern in the top region and by a relatively smooth bottom part. The camera image represents the top view of the process zone. However, the nozzle does not allow to observe the whole melt pool, in particular the melt pool tail, with such an angle of the cutting front.

When the cutting is performed with a lower cutting speed (50 %), the length of the process zone becomes shorter and the melt pool intensity decreases significantly, which corresponds to the obtained lower photodiode signal. This is the result of the surplus of process energy leading to a straighter cutting front and easier melt removal. When the cutting speed is reduced significantly, the heat input becomes too large and burning defects start to occur, drastically increasing roughness. At the same time, due to the disturbance of the combustion wave generation, the process becomes less stable, leading to the increase of the photodiode signal standard deviation.

In line with the speed decrease effect, cutting faster changes the cutting front such that the proportion of the melt pool along the cutting direction increases. This can mainly be explained by a decrease of the cutting front angle due to the lack of energy. Therefore, an increase of the photodiode signal has been observed. Nevertheless, the cutting front is still stable, thus explaining only slight changes in the photodiode signal standard deviation if compared with the nominal speed. The dross appearance might significantly increase the signal due to additional radiation from the resolidified material. However, since it mainly occurs in the region clipped by the nozzle, a drastic increase of the photodiode signal has not been observed, while it has been more pronounced for flame cutting with CO_2 lasers [16].

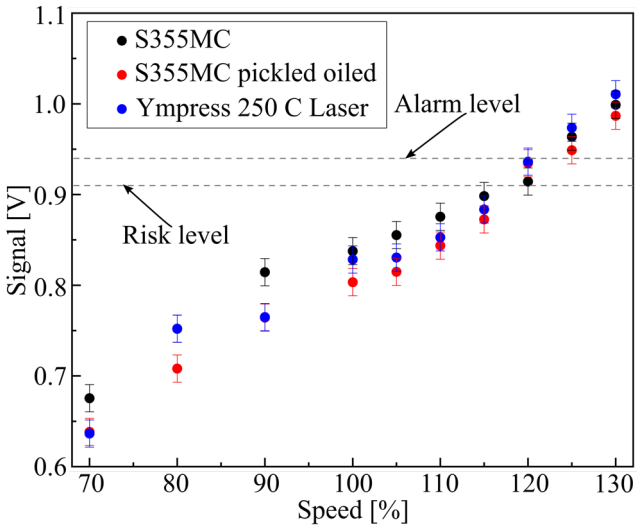

Fig. 7. Average photodiode signal during cutting of 15 mm plates with different cutting speeds.

The robustness of the photodiode signal was examined during cutting of various grades since the chemical composition of the material [17] and the surface condition [18] have a great impact on the cut quality. Therefore, in addition to the different chemical compositions of S355MC and Ympress 250C laser quality grades, S355MC plates without surface finishing, as well as pickled and oiled variants, were cut. The average photodiode signals during cutting of the above-mentioned material grades with speeds 30 % faster and slower than the nominal feed rate (100 %) are shown in Fig. 7.

Despite the difference in material grade, the same trend of the dependence of the photodiode signal from the cutting speed can be noticed. A speed increase leads to a higher signal level caused by the change of the cutting front angle. It should be noted that, even though the cut quality of samples with nominal speed is rather similar (no dross, roughness within 10 % deviation), the dross appearance is slightly different. For S355MC plates without surface finishing, as well as pickled and oiled, limited dross occurs already for cutting with a speed of 125 %, while Ympress 250C laser quality plates could be cut without dross at this speed. Nevertheless, heavy dross or a failed cut situation occurred during cutting with a speed of 130 % for all grades.

One of the main targets of an adaptive control system is to be able to cut at the maximum speed at which the cut quality does not deteriorate. In case of 15 mm mild steel plates, cutting at a speed 20 % faster than the nominal feed rate is possible with even slightly better quality. In this instance, gradual speed increasing before the photodiode signal reaches the risk level can be recommended as a guideline for the control system. When the risk level is reached, it indicates that the risk of unacceptable quality is high and that some precautionary measures should be taken, e.g. a slight speed decrease. The alarm level indicates that the cut quality deterioration is unacceptable and that the process control parameters need to be adapted drastically. In the most severe case, the cut can be completely lost and complete standstill of the cutting is required to correct the process status. These two threshold levels have to be determined for every set of cutting

parameters. In order to detect too slow cutting accompanied by the burning defects occurrence, the signal standard deviation can be used as well.

In order to validate the monitoring setup, flame cutting of mild steel of other thicknesses as well as fusion cutting of stainless steel were performed. Fig. 8 shows average photodiode signals for these experiments. It should be noted that relatively large nozzles are typically used for fusion cutting of thick stainless steel plates (in this case 3.5 mm) which makes the process zone easier to observe in a coaxial monitoring setup and allows transmitting all the radiation from the process towards the sensor.

The same trend as was noticed for 15 mm mild steel can be observed for both 10 mm stainless steel and 8 mm and 10 mm mild steel. Increasing speed results in a photodiode signal level increase induced by the change of the cutting front inclination. However, cutting too fast for stainless steel (e.g. 130 %) leads to signal saturation. This can be explained by the fact that lack of energy significantly changes the cutting front angle causing loss of the full penetration and resulting in an increase of the absorption of the laser beam by the melt layer which enhances the heat transfer to the assist gas. Consequently, instead of dross occurrence as for the flame cutting process, laser-induced plasma might be formed emitting much more light [19].

Another cut quality issue that can occur during flame cutting of thick plates is heat accumulation. Due to conductive heat losses during cutting, the temperature of the base material can rise significantly, enlarging the risk of quality deterioration due to preheating effects [20]. In the most severe cases, the overheating can even result in the occurrence of dross leading to loss of cut. This effect is particularly pronounced for cutting with oxygen, where the level of heat conduction loss is higher, which might lead to strong process limitations especially for nesting and tool path solutions.

In order to test the monitoring setup for the preheating effect, a test part geometry was chosen in such a way as to gradually accumulate heat on each subsequent cutting interval. The cutting was performed according to the sequence of the line numbers provided in Fig. 9. The length of each linear cut is 100 mm with a distance of 5 mm between the lines.

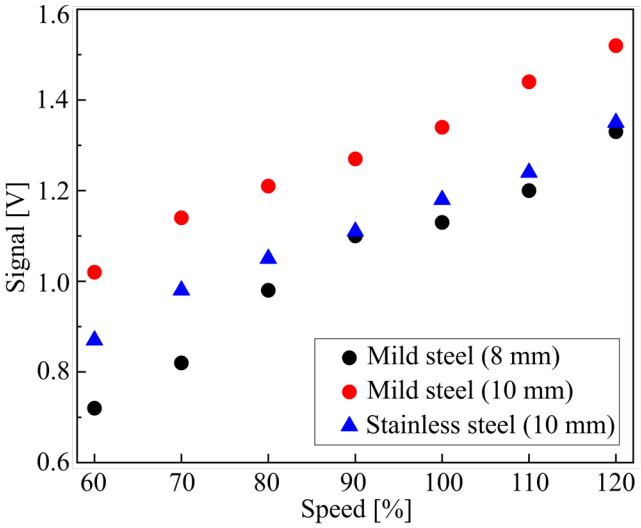

Fig. 8. Average photodiode signal during cutting of mild steel and stainless steel plates with different cutting speeds.

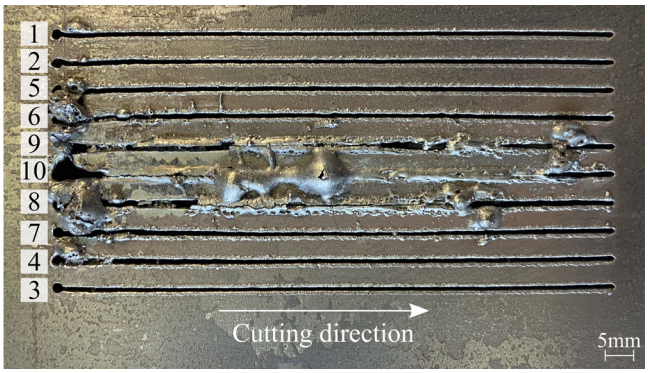

Fig. 9. Bottom view of a sample obtained by cutting a 15 mm S355MC plate with nominal speed showing no cut through in the most preheated regions.

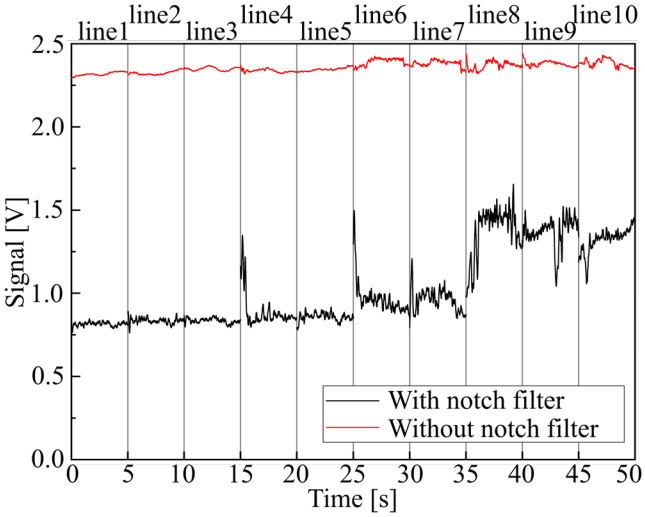

Fig. 10. Photodiode signals during cutting of a 15 mm S355MC plate with consecutive levels of heat accumulation.

The corresponding photodiode signals with and without using the notch filter are depicted in Fig. 10. The signals during the piercings for each line were removed for better visualization. Despite the fact that the temperature of the solid material around the melt pool should considerably increase due to the preheating effect, the sensor only captures radiation from the liquid metal or the resolidified material at a high temperature.

The signal level while using the notch filter starts to slightly rise for lines 6 and 7 which are characterized by considerable quality deterioration. Since piercing is a source of additional heat accumulation as well, the first significant quality degradation could be observed at the zones close to piercings corresponding to the signal peaks at the beginning of line 4 and line 6 related to unstable cutting at these regions. Furthermore, the signal is significantly higher from line 8 onward if compared with the previous lines. Despite the fact that occurrence of dross is unstable, leading to signal variation, the average signal during the cutting of each line undergoes an increase of 10 % for line 6 and line 7 and more than 50 % for lines 8, 9 and 10 compared to line 1. Moreover, the signal deviation is more pronounced at the lines where dross appears.

The experiment without using the notch filter was conducted in order to estimate the influence of laser back reflection on the obtained signal. Due to the high radiation intensity even after passing the dichroic mirror, an amplification eight times less than for other experiments was used for the test in order to

avoid signal saturation. Nevertheless, no significant changes in the photodiode signal level were observed especially when comparing with the results obtained with the notch filter. However, the signal deviation becomes higher starting from line 6 where quality deterioration appears. It might be concluded that the inclination angle of the cutting front does not significantly change while cutting in preheated regions since the signal with laser back reflection does not show any distinction between different lines. That can be used by the adaptive control system to detect the difference between cutting too fast and cutting in preheated areas.

A possible explanation of this result could be that due to the preheating effect the melt pool area expands and the material amount that has to be removed increases. At the same time, the melt pool and heat affected zone temperatures change which has a strong effect on the radiation intensity according to Planck`s and Wien`s laws. This difference in the measured signals becomes more evident when dross appears because the additional resolidified material has a lower temperature emitting even more radiation in the near-infrared spectral range.

4. Conclusion

The InGaAs photodiode signal rises with increasing speed since the inclination angle of the cutting front changes. Such a trend has been observed for different material grades as well as for flame cutting of mild steel with 8 mm and 10 mm thicknesses and fusion cutting of 10 mm stainless steel. Furthermore, the photodiode signal can be used to detect full penetration during piercing in order to reduce the overall piercing time.

The nozzle borders do not allow to observe the melt pool tail during flame cutting of thick plates which obstructs the opportunity to directly observe the appearance of dross. Therefore, the monitoring system is based on sensing parameters such as signal level and standard deviation that correlate with the cut quality but do not directly measure it.

The developed monitoring setup allows verifying the maximum cutting speed at which the cut quality does not degrade as well as detecting cutting in preheated regions. However, the threshold levels have to be adjusted for every material-thickness combination in order to couple the system with adaptive control.

References

[1] Kek T, Grum J. AE signals as laser cutting quality indicators. Insight Non-Destructive Test Cond Monit 2009; 51:3:124-128.
[2] Chen L-S. In-process monitoring of the cutting front of CO_2 laser cutting with off-axis optical fibre. Int J Adv Manuf Tech 1997; 13:10:685–691.
[3] Wen P, Zhang Y, Chen W. Quality detection and control during laser cutting progress with coaxial visual monitoring. J Laser Appl 2012; 24:3:032006.
[4] Purtonen T, Kalliosaari A, Salminen A. Monitoring and adaptive control of laser processes. Phys Procedia 2014; 56:1218-1231.
[5] You DY, Gao XD, Katayama S. Review of laser welding monitoring. Science and Technology of Welding and Joining 2014; 19:3:181-201.
[6] Everton SK, Hirsch M, Stravroulakis P, Leach RK, Clare AT. Review of in-situ process monitoring and in-situ metrology for metal additive manufacturing. Mater Des 2016; 95:431-445.
[7] Liu S, Farahmand P, Kovacevic R. Optical monitoring of high power direct diode laser cladding. Opt Laser Technol 2014; 64:363-376.
[8] Adelmann B, Schleier M, Neumeier B, Hellmann R. Photodiode-based cutting interruption sensor for near-infrared lasers. Appl Opt 2016; 55:7:1772-1778.
[9] Schleier M, Adelmann B, Neumeier B, Hellmann R. Burr formation detector for fiber laser cutting based on a photodiode sensor system. Opt Laser Technol 2017; 96:13-17.
[10] Schleier M, Adelmann B, Esen C, Hellmann R. Cross-correlation-based algorithm for monitoring laser cutting with high-power fiber lasers. IEEE Sens J 2018; 18:4:1585-1590.
[11] Garcia SM, Ramos J, Lamikiz A, Figueras J. Influence of process parameters in laser piercing. Appl Opt 2019; 9:3231.
[12] Dubrov AV, Dubrov VD, Zavalov YN, Panchenko VY. Application of optical pyrometry for on-line monitoring in laser-cutting technologies. Appl Phys B Lasers Opt 2011; 105:537-543.
[13] Garmendia I, Ocaña R, Soriano C, Lambarri J. Optical monitoring of fiber laser based cutting processes for in-situ quality assurance. In: Proceedings of Lasers in Manufacturing Conference 2017.
[14] Duflou JR, Fallahi Sichani E, De Keuster J, Kruth J-P. Development of a real time monitoring and adaptive control system for laser flame cutting. In: Proceedings of ICALEO 2009; 527-536.
[15] Levichev N, Costa Rodrigues G; Tomás García A; Duflou JR. Trim-cut technique for analysis of melt flow dynamics in industrial laser cutting machine. Procedia CIRP (accepted).
[16] De Keuster J, Duflou JR, Kruth J-P. Monitoring of high-power CO_2 laser cutting by means of an acoustic microphone and photodiodes. Int J Adv Manuf Technol 2007; 35:115-126.
[17] Nagels E, Duflou JR, Van Humbeeck J. The influence of sulphur content on the quality of laser cutting of steel. J Mater Process Technol 2007; 194:159-162.
[18] Manohar M. CO_2 laser beam cutting of steels: Material issues. J Laser Appl 2006; 18:2:101-112.
[19] Fallahi Sichani E, Kohl S, Duflou JR. Plasma detection and control requirements for CO_2 laser cutting. CIRP Ann – Manuf Technol 2013; 62:215-218.
[20] Levichev N, Costa Rodrigues G, Dewil R, Duflou JR. Anticipating heat accumulation in laser oxygen cutting of thick metal plates. J Laser Appl 2020; 32:022018.